INTERNATIONAL JOURNAL FOR NUMERICAL METHODS IN FLUIDS
Int. J. Numer. Meth. Fluids 2002; **38**:515–531 (DOI: 10.1002/fld.225)

A reappraisal of Taylor–Galerkin algorithm for drying–wetting areas in shallow water computations

M. Quecedo[1,2] and M. Pastor[2,3,*]

[1] *ENUSA, Madrid, Spain*
[2] *Department of Applied Mathematics, ETSI de Caminos, Madrid, Spain*
[3] *Centro de Estudios y Experimentación de Obras Públicas, Madrid, Spain*

SUMMARY

Non-linear shallow water equations are a useful approximation to phenomena such as estuary dynamics, tidal propagation, breaking of a dam, flood waves, etc. Quite frequently they involve propagation over dry beds and drying of wet zones, for which boundary changes. To solve this problem either special techniques such as remeshing and Arbitrary Lagrangian Eulerian formulations or algorithms initially developed for flows exhibiting shocks have been proposed in past years. The purpose of this paper is to show how classical finite elements formulations, such as Taylor–Galerkin can be applied to solve the problem to wetting–drying areas in a simple yet efficient manner. Copyright © 2002 John Wiley & Sons, Ltd.

KEY WORDS: dam-break; drying–wetting; Taylor–Galerkin

1. INTRODUCTION

Some very efficient finite element schemes have been proposed in the past years for convection dominated problems. Among them, two efficient alternatives are the so-called Taylor–Galerkin [1–3] and Characteristics-Based Galerkin [4–6] formulations. They have been successfully applied to a great variety of problems, such as pollutant transport, compressible and incompressible fluid dynamics problems, and also to coastal and river mechanics phenomena. In the latter case, it is possible to make some assumptions which lead to what is known as shallow water or depth-integrated equations.

As in many non-linear fluid dynamics problems, shocks and discontinuities can be produced. One of the most interesting and demanding problems, both from the practical and the numerical points of view, is that of breaking of a dam. This problem may involve, depending on whether the flood wave propagates over a dry or a 'wet' bottom, difficulties arising either from the existence of moving boundaries or from propagation of a shock.

*Correspondence to: M. Pastor, Edificio CETA, CEDEX, Alfonso XII, 3Y5, 28014 Madrid, Spain.

Received 15 November 2000
Revised 5 April 2001

To solve the latter, special algorithms initially developed for high-speed flows exhibiting shocks have become more widespread in the past years, as they are claimed to provide higher resolution at shocks [7–10].

In a recent paper by Satya Sai *et al.* [11] the performance of specialized and classical algorithms on high-speed problems with shocks was compared, with the result that general purpose algorithms provided a satisfactory approach.

The purpose of this paper is to extend these results to the special case of catastrophic flood waves, verifying that classical yet robust finite element algorithms are still attractive alternatives.

The paper is structured as follows. First of all, the depth-averaged equations are presented. The formulation here differs from those that have been previously used with both Taylor–Galerkin [2, 3] and Characteristic-Based-Galerkin [6] algorithms. Then, the Taylor–Galerkin algorithm will be used to discretize the depth-integrated equations. Following this section, we will present a comparison with the analytical solutions which exist for the dam-break problem over both dry and wet beds. Finally, several applications to real problems such as breaking of a dam, water supply deposits and flow slides will be presented.

Depth-averaged models provide an attractive alternative which reduces the computational cost. Here, the variables reduce to depth of flow and two-dimensional velocities. Still, the problem of propagation over dry areas remains, and adaptive remeshing and Arbitrary Lagrangian Eulerian (ALE) techniques have been proposed [12] to follow the domain occupied by the fluid. There, a classical general-purpose Characteristics-Based Galerkin finite element scheme was used.

2. MATHEMATICAL MODEL

The model used in this paper for solving the free surface flow problem is based on the solution of the shallow water equations.

These equations are obtained from the Navier–Stokes equations considering an incompressible, isothermal fluid and assuming that the vertical component of the acceleration is negligible. Furthermore, the contribution of the viscous forces is also typically neglected. The shallow water governing equations are finally obtained by depth integrating the resulting mass and momentum conservation equations. The details of the derivation can be found in standard text books [13, 14].

Using the notation described in Figure 1, the shallow water equations are:

$$\frac{\partial h}{\partial t}+\frac{\partial}{\partial x}(uh)+\frac{\partial}{\partial y}(vh)=0$$

$$\frac{\partial}{\partial t}(uh)+\frac{\partial}{\partial x}(u^2h)+\frac{\partial}{\partial y}(uvh)=-gh\frac{\partial \eta}{\partial x}+\tau_{s,x}-\tau_{b,x}+r_x-\frac{h}{\rho}\frac{\partial p_a}{\partial x}$$

$$\frac{\partial}{\partial t}(vh)+\frac{\partial}{\partial x}(uvh)+\frac{\partial}{\partial y}(v^2h)=-gh\frac{\partial \eta}{\partial y}+\tau_{s,y}-\tau_{b,y}+r_y-\frac{h}{\rho}\frac{\partial p_a}{\partial y}$$

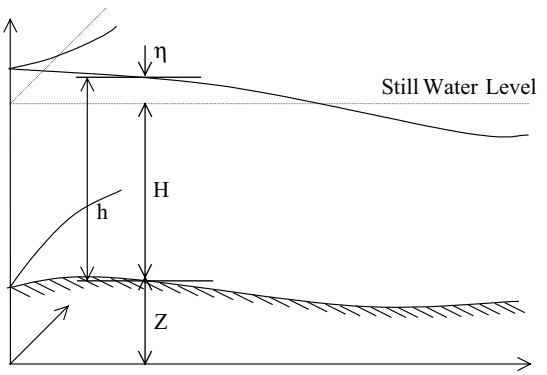

Figure 1. Shallow water problem notation.

where u, v are the components of the depth averaged velocity; $\boldsymbol{\tau}_s$ and $\boldsymbol{\tau}_b$ are the free surface (wind) and bottom (friction) traction vectors; $\mathbf{r}$ is the Coriolis force vector; p_a is the atmospheric pressure; and ρ is the fluid density.

These equations are written in a compact form as:

$$\begin{aligned} &\frac{\partial h}{\partial t} + \operatorname{div}(\mathbf{U}) = 0 \\ &\frac{\partial \mathbf{U}}{\partial t} + \operatorname{div}(\mathbf{u} \otimes \mathbf{U}) = -gh\, grad\, \eta + \boldsymbol{\tau}_s + \boldsymbol{\tau}_b + \mathbf{r} - \frac{h}{\rho} grad\ p_a \end{aligned} \tag{1}$$

where $\mathbf{U} = \mathbf{u}h$.

For the sake of simplicity and without loss of generality, the contribution to the source term from the Coriolis force, the wind tractions and the atmospheric pressure gradients are ignored in future derivations.

With regard to the bottom friction, $\boldsymbol{\tau}_b$, either the usual Chezy–Manning formula which, after depth integration and divided by the fluid density, is

$$\boldsymbol{\tau}_b = \frac{gn^2|\mathbf{u}|\mathbf{u}}{h^{1/3}} \tag{2}$$

or more complex ones, as those used in debris flow analyses [15],

$$\boldsymbol{\tau}_b = \frac{\mathbf{c}}{\rho} + gh\, \tan\phi \frac{\mathbf{u}}{|\mathbf{u}|} + \frac{gn^2\mathbf{u}|\mathbf{u}|}{h^{1/3}}$$

can be considered.

However, as a $grad\, \eta$ component exists, Equation (1) is not written in a conservative form. Therefore, numerical methods used to solve conservation laws written in the conservative form, such as the Taylor–Galerkin method, are not applicable to solve these equations in their current state.

To achieve this goal, Equation (1) is rewritten by considering that

$$-gh\, grad\, \eta = -grad\left(g\frac{h^2 - H^2}{2}\right) + g(h - H)\, grad\, H$$

which results in

$$\begin{gathered}\frac{\partial h}{\partial t}+\operatorname{div}(\mathbf{U})=0\\ \frac{\partial \mathbf{U}}{\partial t}+\operatorname{div}\left(\mathbf{u}\otimes\mathbf{U}+\left(g\frac{h^2-H^2}{2}\right)\underline{\mathbf{1}}\right)=g(h-H)\,grad\,H+\boldsymbol{\tau}_b\end{gathered}\tag{3}$$

where $\underline{\mathbf{1}}$ is the unit tensor.

Now, by introducing

- $\boldsymbol{\phi}=\begin{Bmatrix}\mathrm{h}\\ \mathrm{U}_x\\ \mathrm{U}_y\end{Bmatrix}$
- $\mathrm{F}_x=\begin{Bmatrix}\mathrm{U}_x\\ \mathrm{u}_xU_x+g\dfrac{h^2-H^2}{2}\\ \mathrm{u}_yU_x\end{Bmatrix}\quad \mathrm{F}_y=\begin{Bmatrix}\mathrm{U}_y\\ \mathrm{u}_xU_y\\ \mathrm{u}_yU_y+g\dfrac{h^2-H^2}{2}\end{Bmatrix}$
- $\mathbf{S}=\begin{Bmatrix}0\\ \mathrm{g}(h-H)\dfrac{\partial H}{\partial x}+\tau_{b,x}\\ \mathrm{g}(h-H)\dfrac{\partial H}{\partial x}+\tau_{b,y}\end{Bmatrix}$

these equations can be cast in the conservative form as

$$\frac{\partial\boldsymbol{\phi}}{\partial t}+\operatorname{div}\underline{\mathbf{F}}=\mathbf{S}\tag{4}$$

This $h-\eta$ formulation is the basis for the solution of coastal hydrodynamics problems using the FEM [2, 13].

The same purpose of writing the shallow water equations in a conservative form can be achieved by considering, see Figure 1, that

$$grad\,\eta=grad(h+Z)$$

resulting now in

$$\begin{gathered}\frac{\partial h}{\partial t}+\operatorname{div}(\mathbf{U})=0\\ \frac{\partial \mathbf{U}}{\partial t}+\operatorname{div}\left(\mathbf{u}\otimes\mathbf{U}+g\frac{h^2}{2}\underline{1}\right)=-gh\,grad\,Z+\boldsymbol{\tau}_b\end{gathered}\tag{5}$$

In this case, the flux tensor and the source vector are

- $\mathbf{F}_x=\begin{Bmatrix}\mathrm{U}_x\\ \mathrm{u}_xU_x+g\dfrac{h^2}{2}\\ \mathrm{u}_yU_x\end{Bmatrix}\quad \mathbf{F}_y=\begin{Bmatrix}\mathrm{U}_y\\ \mathrm{u}_xU_y\\ \mathrm{u}_yU_y+g\dfrac{h^2}{2}\end{Bmatrix}$

- $\mathbf{S} = \begin{Bmatrix} 0 \\ gh\dfrac{\partial Z}{\partial x} + \tau_{b,x} \\ gh\dfrac{\partial Z}{\partial y} + \tau_{b,y} \end{Bmatrix}$

This formulation does not require knowledge of the value of H, hence the still water level (SWL). This point could be an issue in problems involving drying–rewetting. Thus, this formulation is more appropriate for the analyses of dam break, debris flow problems etc., while it can be used also for coastal engineering problems. For these reasons, this *h-Z* formulation has been retained in this paper. However, as the reader will notice, the numerical method developed in the next section is applicable for both formulations as it only requires to incorporate the corresponding expression for the flux tensor, $\underline{\mathbf{F}}$, and source vector, $\mathbf{S}$.

3. NUMERICAL METHOD

There are a number of methods available within the FEM context to solve advection problems as those governed by Equation (4), see for instance Reference [13]. Within these methods, the Taylor–Galerkin procedure forwarded by Donea *et al.* [1, 16] was further developed and applied by Peraire [2, 3] to the solution of the shallow water equations.

The Taylor–Galerkin algorithm can be considered as the FEM counterpart of the Lax–Wendroff procedure in the FDM. It basically consists of a higher order expansion of the time derivative, followed by the spatial discretization of the resulting equation using the conventional Galerkin weighting method.

However, following the general procedure—see Reference [13] for a detailed derivation—requires the calculation of the derivatives of the flux tensor, $\underline{\mathbf{F}}$, and source vector, $\mathbf{S}$, relative to the vector of unknowns, $\boldsymbol{\phi}$, for each element in the mesh and performing a number of matrix multiplications.

To avoid this computer memory and time consuming operations Peraire, [2], developed a two-step algorithm that can be regarded as the FEM implementation of the Richtmyer scheme [17]. Globally, the Richtmyer scheme is of second-order accuracy in space and time [18]. Due to its accuracy and simplicity it has been used by the authors to solve the shallow water equations. For this reason, the next section describes the two-step algorithm.

3.1. Two-step Taylor–Galerkin algorithm

As introduced earlier, the Taylor–Galerkin procedure for solving Equation (4) starts from a second-order expansion in time

$$\boldsymbol{\phi}^{n+1} = \boldsymbol{\phi}^n + \Delta t \left.\frac{\partial \boldsymbol{\phi}}{\partial t}\right|^n + \frac{1}{2}\Delta t^2 \left.\frac{\partial^2 \boldsymbol{\phi}}{\partial t^2}\right|^n \tag{6}$$

where the first-order time derivative of the unknowns can be calculated using Equation (4)

$$\left.\frac{\partial \boldsymbol{\phi}}{\partial t}\right|^n = (\mathbf{S} - \operatorname{div} \underline{\mathbf{F}})^n$$

To obtain the second-order time derivative, the two-step Taylor–Galerkin procedure considers an intermediate step between t^n and t^{n+1}. The aim of this first time step is to calculate the solution at a time $t^{n+1/2}$. This step is followed by a second one that brings the solution to t^{n+1}.

In this way, the first step results in

$$\boldsymbol{\phi}^{n+1/2} = \boldsymbol{\phi}^n + \frac{\Delta t}{2}(\mathbf{S} - \operatorname{div} \underline{\mathbf{F}})^n \tag{7}$$

which allows the calculation of $\underline{\mathbf{F}}^{n+1/2}$ and $\mathbf{S}^{n+1/2}$.

Considering now a Taylor series expansion of the flux and source terms,

$$\underline{\mathbf{F}}^{n+1/2} = \underline{\mathbf{F}}^n + \left(\frac{\partial \underline{\mathbf{F}}}{\partial t}\right)^n \frac{\Delta t}{2}$$

$$\mathbf{S}^{n+1/2} = \mathbf{S}^n + \left(\frac{\partial \mathbf{S}}{\partial t}\right)^n \frac{\Delta t}{2}$$

and the values of $\underline{\mathbf{F}}^{n+1/2}$ and $\mathbf{S}^{n+1/2}$, the flux and sources time derivatives are calculated as

$$\left(\frac{\partial \underline{\mathbf{F}}}{\partial t}\right)^n = \frac{2}{\Delta t}(\underline{\mathbf{F}}^{n+1/2} - \underline{\mathbf{F}}^n)$$

$$\left(\frac{\partial \mathbf{S}}{\partial t}\right)^n = \frac{2}{\Delta t}(\mathbf{S}^{n+1/2} - \mathbf{S}^n)$$

Incorporating these expressions into the second-order time derivative

$$\left.\frac{\partial^2 \boldsymbol{\phi}}{\partial t^2}\right|^n = \frac{\partial}{\partial t}(\mathbf{S} - \operatorname{div} \underline{\mathbf{F}})^n$$

results in

$$\left.\frac{\partial^2 \boldsymbol{\phi}}{\partial t^2}\right|^n = \frac{2}{\Delta t}(\mathbf{S}^{n+1/2} - \mathbf{S}^n - \operatorname{div}(\underline{\mathbf{F}}^{n+1/2} - \underline{\mathbf{F}}^n))$$

Now replacing the expressions for the first- and second-order time derivatives in the Taylor series expansion (Equation (6)), allows the determination of the unknowns at time t^{n+1}

$$\boldsymbol{\phi}^{n+1} = \boldsymbol{\phi}^n + \Delta t(\mathbf{S}^{n+1/2} - \operatorname{div} \underline{\mathbf{F}}^{n+1/2})$$

This equation is spatially discretized using conventional Galerkin weighting to finally result in the system of equations to be solved to obtain the unknown increments in the variables at the time step:

$$\underline{\mathbf{M}}\Delta\boldsymbol{\phi} = \Delta t \left(\int_\Omega \underline{\mathbf{N}}\mathbf{S}^{n+1/2}\,\mathrm{d}\Omega - \int_{\Gamma_N} \underline{\mathbf{N}}\mathbf{F}^{n+1/2}\,\mathrm{d}\Omega + \int_\Omega \underline{\mathbf{F}}^{n+1/2}\, grad\, \underline{\mathbf{N}}\,\mathrm{d}\Omega\right) \tag{8}$$

3.2. Algorithmic aspects

3.2.1. Equation system solution. A system of equations

$$\underline{\mathrm{M}}\mathbf{x} = \mathbf{f}$$

can be economically solved using a Jacobi iteration scheme

$$\mathbf{x}^{(k+1)} = \mathbf{x}^{(k)} + M_L^{-1}(\mathbf{f} - \underline{\mathrm{M}}\mathbf{x}^{(k)})$$

where the superscript k is the iteration counter, if an approximate inverse matrix, M_L^{-1}, is known in advance.

As in the case of Equation (8) an approximate inverse of the system matrix, $\underline{\mathbf{M}}$, is the lumped mass matrix, the equation system (8) can be solved using this algorithm. Typically, less than six iterations are enough to obtain an accurate solution.

3.2.2. Allowed time step. The above-described explicit algorithm is conditionally stable. To ensure stability, the Courant number corresponding to the maximum velocity of propagation has to fulfil the condition [2]

$$C = \frac{|\mathbf{u}| + c}{h_e}\Delta t \leqslant \alpha$$

where

- $\alpha = 1$ for the lumped mass matrix and $\alpha = 1/\sqrt{3}$ for the consistent mass matrix,
- $c = \sqrt{gh}$ is the wave speed of propagation and,
- h_e is a typical element length.

Thus, the convection component sets the constraint

$$\Delta t_{CV} \leqslant \alpha \frac{h_e}{|\mathbf{u}| + c} \tag{9}$$

Besides, another limitation is derived from the source term [2],

$$\frac{C}{S_r} \leqslant 2$$

where S_r is the source number defined as

$$S_r = \frac{|\mathbf{u}| + c}{|\mathbf{S}|/|\mathbf{V}|h_e}$$

Neglecting the contribution to the source number of the bed slope and considering the Chezy–Manning bed resistance described by Equation (2), the corresponding maximum time allowed from the source term is

$$\Delta t_{SR} \leqslant \frac{2h^{4/3}}{gn^2|\mathbf{u}|} \tag{10}$$

Therefore, the maximum time step allowed to ensure algorithm stability is

$$\Delta t = \min(\Delta t_{cv}, \Delta t_{sr}) \tag{11}$$

Finally, it has to be pointed out that in order to improved the accuracy and smooth out of oscillations [13], the calculation of the unknowns at time $t^{n+1/2}$ (Equation (7)), performed at the element level uses the optimum time step value given by Equation (9). This optimal value is calculated and used for each element in turn, while the minimum of Equation (11), calculated for the whole mesh, is used in Equation (8) to ensure overall scheme stability.

3.2.3. Wetting and drying areas. One of the major issues that can be involved when solving problems governed by the shallow water equations is the handling of drying and wetting areas.

A simple solution, useful when a single element can accommodate the elevation changes, has been proposed by Lynch and Gray [19]. It consists in repositioning the nodes located at the boundary along its normal as required by the elevation changes. In those cases involving variations that cannot be accommodated by a single element and topological problems arise, remeshing is necessary.

Another possibility consists in turning on and off the elements and preserving the mass in the process. This could be achieved by using the method suggested by Peraire [2]. He proposed to use the nodal values of the variables to perform the interpolations within the elements and to extend the area integrals only to the flooded area of each element. This procedure requires accurate knowledge of the position of the boundary after each time step. However, nothing is said on this key point by Peraire.

To solve the issue of the interface position, the level set technique proposed by Sethian [20], with the reinitialization used by Sussman *et al.* [21], can be used. This technique has been successfully used by the authors in the solution of two-phase flows [22] of fluids of a general type. It has also been checked by the authors that, within the shallow water context, this technique provides an accurate determination of the flood-to-dry boundary position.

However, in most of the problems, the accuracy, and expense, brought into the solution by incorporating the level set procedure to the problem solution would be unnecessary. Therefore, in the examples shown in the next section, the authors followed the much simpler method of interpolation within the elements using the nodal variables, considering a null value for the variables corresponding to dry nodes. In this way, calculations to accurately determine the position of the boundary within the partially dried–flooded elements are not done.

It is worth mentioning that considering a null value for the water depth, h, is not allowed, unless special precautions are taken, by methods using a pressure-like variable instead of the water depth, such as the CBG, where the following change of variables is done [6]

$$p \equiv \tfrac{1}{2} g(h^2 - H^2)$$

Incorporating this pseudo-pressure in the continuity equation

$$\frac{\partial h}{\partial t} + \operatorname{div}(\mathbf{U}) = 0$$

this equation becomes

$$\frac{1}{gh}\frac{\partial p}{\partial t} + \operatorname{div}(\mathbf{U}) = 0$$

where numerical difficulties are found when h is closed or equal to zero.

Finally, it is necessary to indicate that an interesting alternative has been recently proposed in Reference [12]. It consists of using an ALE formulation joint to mesh adaptive refinement.

4. NUMERICAL EXAMPLES

The purpose of this section is to present several examples which show how the simple changes introduced in the formulation allow modelling of phenomena such as drying–wetting areas and shock propagation, which have not been dealt with before using the Taylor–Galerkin algorithm. Therefore, the examples presented next are aimed at bringing new insights in the performance of the algorithm rather than to prove the algorithm performance itself. All these numerical examples have been solved using the *h-Z* formulation of the shallow-water equations and the algorithm presented above.

It was mentioned in the introduction that there exist *ad-hoc* methods for such purposes such as Riemann solvers and ALE formulations plus mesh refinement. However, the Taylor–Galerkin algorithm presents an excellent compromise between simplicity of formulation and accuracy.

Of course, the Taylor–Galerkin (TG) method is not the unique classical finite element algorithm, and in the past years some improvements have been proposed. For instance, it is worth mentioning here the Characteristic-Based Galerkin (CBG) method proposed in References [4–6].

The reason of having chosen TG instead of CBG lies in the smaller dissipation presented by the former. This will be illustrated in the first example.

4.1. Free oscillation of a sinusoidal wave

The first numerical example illustrates the dissipation performance of the two-step Taylor–Galerkin algorithm. The example concerns a long rectangular channel where an initially sinusoidal wave is left free to oscillate.

The channel dimensions are 800×80 m and the still water level is 8 m. Null bottom friction is considered. The mesh comprises 375 nodes grouped in 628 linear triangles, see Figure 2. The normal velocities along the boundary are set to zero.

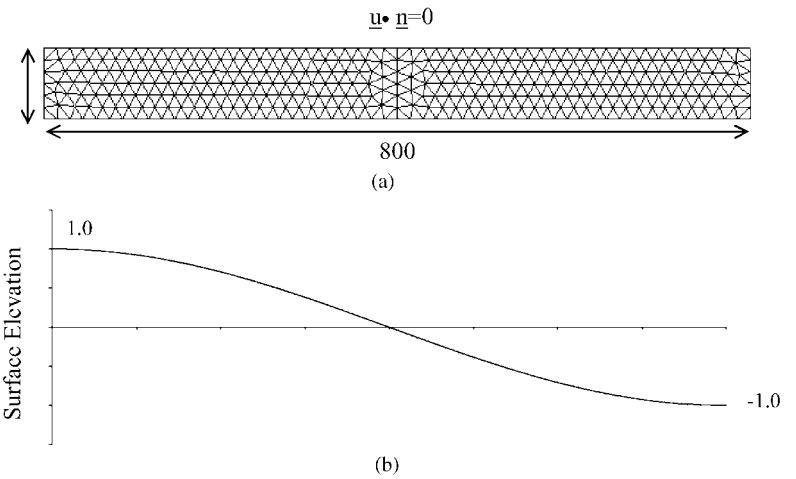

Figure 2. Free oscillation of a sinusoidal wave: (a) mesh; and (b) initial surface elevation.

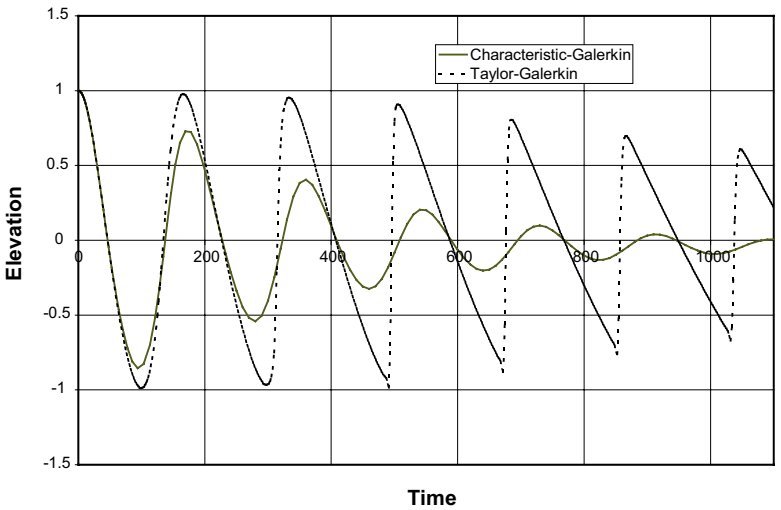

Figure 3. Evolution of the calculated elevation on the vertical walls of the channel using the Taylor–Galerkin and the Characteristic-Based Galerkin algorithms.

The initial condition consists of an imposed surface elevation described by

$$\eta(x, t=0) = \cos\left(2\pi \frac{x}{1600}\right)$$

that it is freely left to move by the acting gravity.

Figure 3 depicts the time evolution of the calculated elevation at the nodes located at the left vertical wall. For comparison, the corresponding results obtained using an implicit Characteristic-Based Galerkin procedure [6] are included in this figure.

The reduction of the wave amplitude observed in this figure, indicates that the Taylor–Galerkin algorithm suffers numerical dissipation and that this dissipation is much smaller than the corresponding to the Characteristic-Based Galerkin method.

Another point suggested by this figure is that in the case of the Taylor–Galerkin algorithm, non-linear effects distort the initially sinusoidal wave given rise, as time advances, to a bore.

Figure 4 shows the surface elevation along the channel length at time zero and at $t = 1200$, revealing this effect. If a smaller wave amplitude, such as 0.2, than that used in this example, 2.0, is used, the initially sinusoidal wave maintains its shape through the calculations. Due to the higher damping introduced by the CBG procedure, the ratio between the surface elevation and the depth becomes increasingly smaller making non-linear effects negligible in this case as it is clear from Figure 3.

4.2. Flood waves over dry and wet bottoms

We will consider next two one-dimensional problems for which analytical solutions exist. A one-dimensional channel of 2000 m length contains a dam situated at $x = 1000$ m, filled with water of constant depth of 10 m, as it can be seen in Figure 5. It has been assumed that the bottom is horizontal, and that no friction exists.

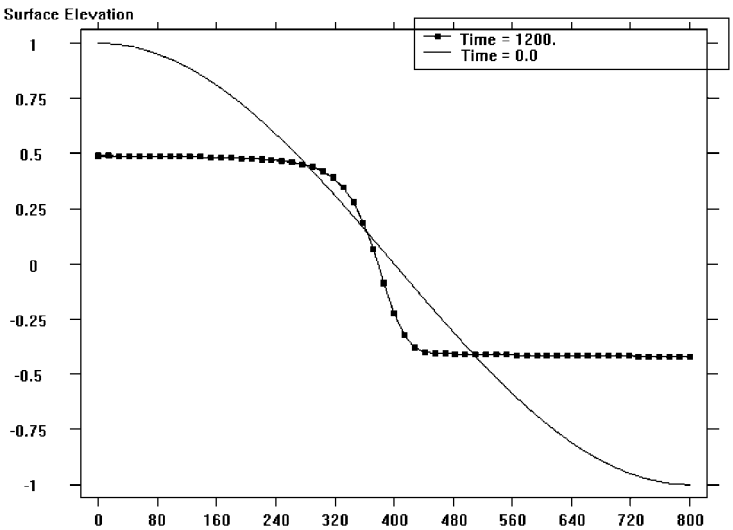

Figure 4. Surface elevation calculated using the Taylor–Galerkin procedure at two time steps, showing the development of a bore.

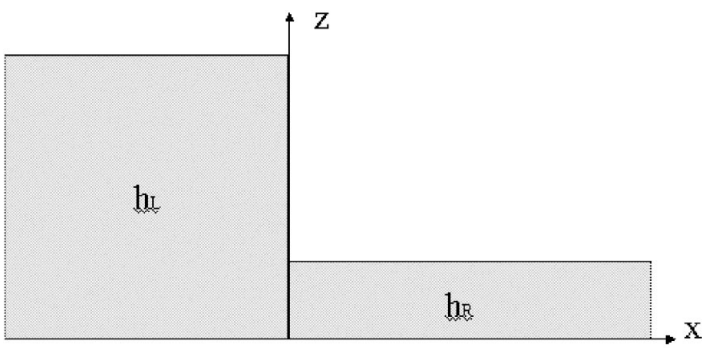

Figure 5. One-dimensional dam problem.

The nature of the solution depends on whether the bottom on the right-hand side has water or not. In the first case, solution consists of the propagation of a shock to the right, together with a rarefaction wave, while in the second case the solution consists of one rarefaction wave with speeds of $\sqrt{gh_L}$ (head) and $-2\sqrt{gh_L}$ (toe).

The first case can be used to illustrate how the TG algorithm performs in the propagation of a shock. Figure 6 presents both the analytical and the computed solution.

4.3. Propagation of a rectangular hump on a slope

This example tests the drying and wetting capabilities of the algorithm. In this example a rectangular hump of water is placed at the middle of a long rectangular channel and left free to move.

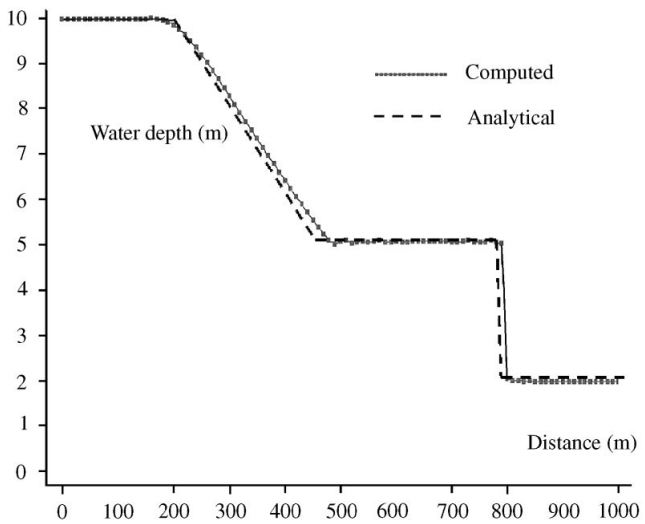

Figure 6. Propagation over a wet bottom.

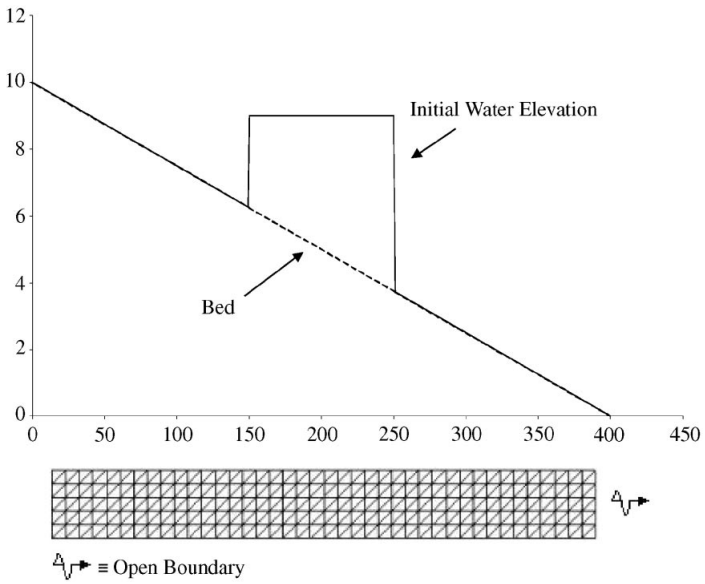

Figure 7. Propagation of a rectangular hump on a slope. Problem layout.

The channel bed is considered frictionless with slope 2.5 per cent. The hump height and width are 4 m, at its mid position, and 100 m respectively. The remaining domain is initially dry.

Figure 7 depicts the problem layout and the mesh used to discretize the domain. The mesh comprises 246 nodes forming 400 three-node triangles. Reflective, i.e. $\bar{v} \cdot \bar{n} = 0$, boundary

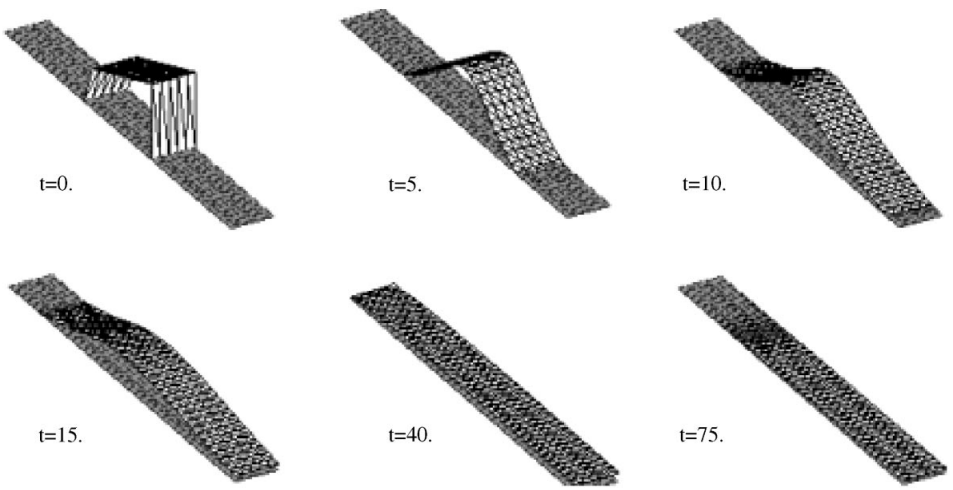

Figure 8. Propagation of a rectangular water hump on a slope.

conditions are prescribed on the channel walls with exception of the right vertical wall, where open boundary conditions are used.

Figure 8 presents the evolution of the water elevation. It is observed that the water front initially moves up and downwards, flooding dry nodes. Once the maximum Z has been reached and the front moves downwards, wet nodes become dried. Finally, as expected, all the domain becomes dry.

4.4. Collapse of a water column

The next example concerns the collapse of a conical water column. Although during the first instants of the column collapse, vertical accelerations need to be considered, once the horizontal velocities are dominant, the shallow water equations provide a good approximation to the problem solution.

The cone has a total height over the horizontal ground of 10 m and 1 m diameter. It is located in the centre of an square domain of 5 m length. Figure 9 depicts the problem layout. The mesh is composed of 2949 nodes arranged in 5696 three-node triangles.

In order to get a bore and to qualitatively assess the performance of the Taylor–Galerkin h-Z formulation, a non-zero still water level, 0.5 m, has been considered. Finally, the problem incorporates bottom friction using the Chezy–Manning resistance (Equation (2)), with coefficient $n = 0.1$.

Figure 10 depicts the free surface elevations at different times. These results are deemed as qualitatively reasonable.

4.5. Broken dam

The last example further demonstrates the wetting and drying capabilities of the algorithm. The example concerns the 2D dam-break problem. This problem is typically solved using the shallow water equations although in the case of zero tailwater depth, the non-hydrostatic

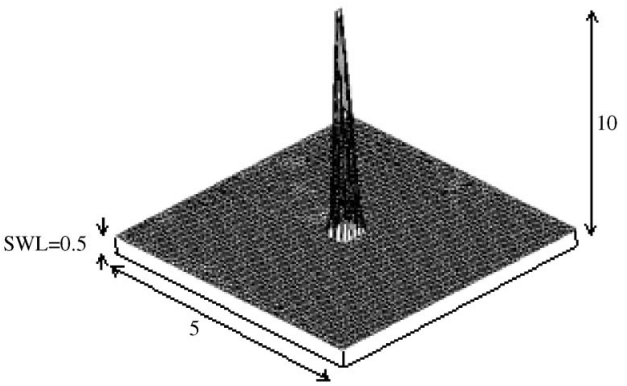

Figure 9. Collapse of a water column. Problem layout.

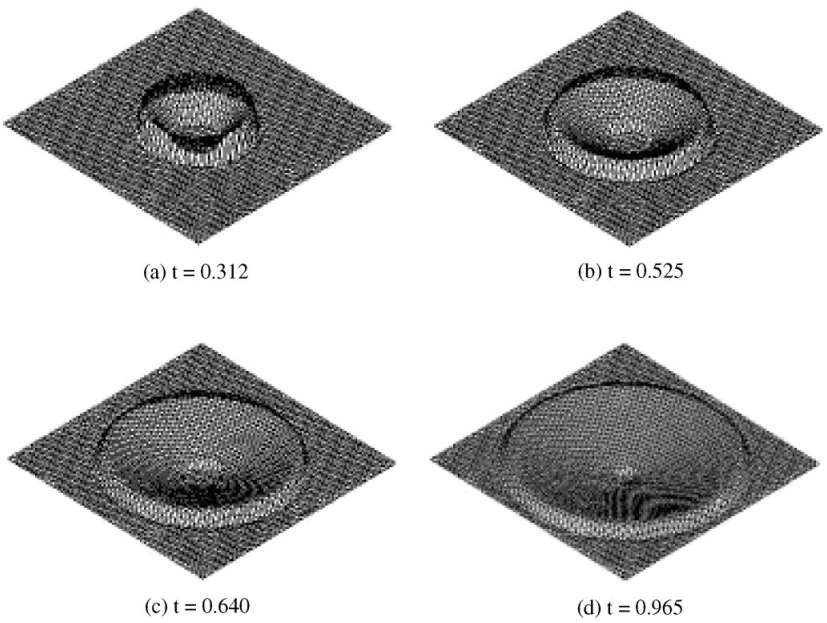

Figure 10. Collapse of a water column. Wave pattern at different times.

pressure distribution existing just at the time the dam breaks, influences the long-term results [23].

Figure 11 depicts the problem layout. The water front is initially located at a horizontal position $x = 110$ m. The breach is 75 m length and it is non-symmetrically located in the dam. The water height in the reservoir is 10 m while downstream is initially dry. The mesh comprises 1844 nodes grouped forming 3476 three-node triangles. Null bottom friction has been considered.

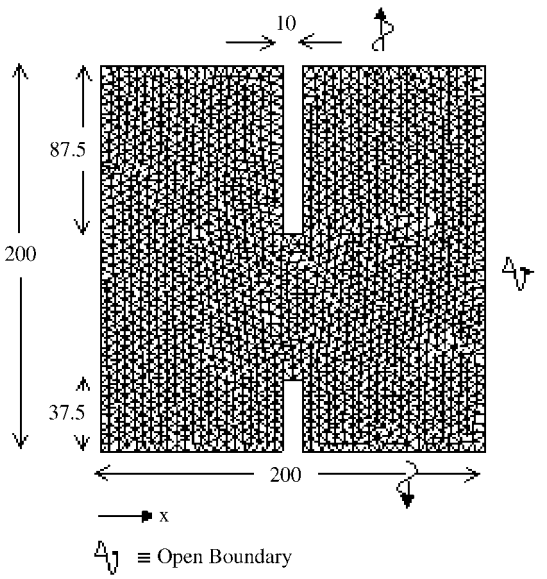

Figure 11. Dam-break problem layout.

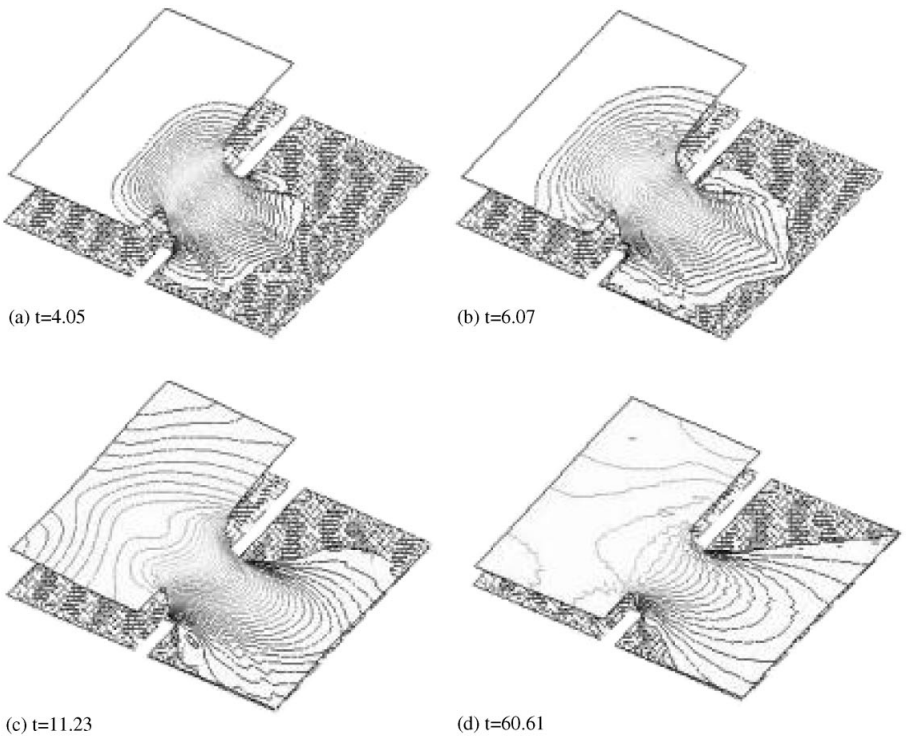

Figure 12. Dam-break problem. Evolution of the water elevation assuming downstream dry bed.

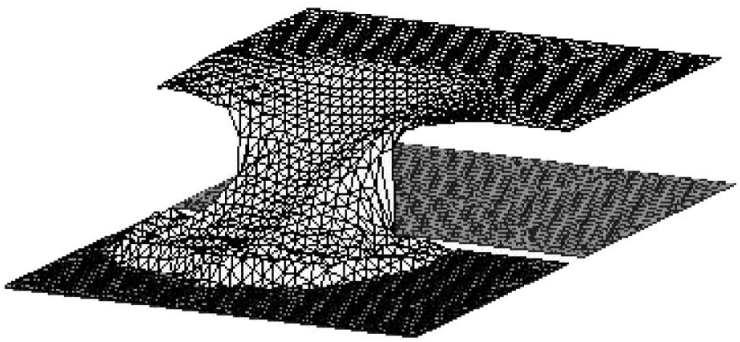

Figure 13. Dam-break problem. Water height calculated at $t = 5.03$ s considering a tailwater depth of 0.1 m.

All the boundaries are considered as reflective, impermeable walls with the exception of the right vertical and horizontal upper and lower boundaries downstream which are considered open boundaries.

Figure 12 depicts the contours of the water elevation for different times during the calculation for dry bed conditions. In this case, dry-bed conditions, as the problem consists of a rarefaction fan, there is a smooth transition in the water depth from the breach to the dry bed.

However, if a small tailwater depth, 0.1 m, is considered, a bore forms and moves downstream, Figure 13.

This results agree with those reported in the literature using more sophisticated methods, see for instance References [8, 9, 24].

5. CONCLUSIONS

The discretization with the Taylor–Galerkin algorithm of the proposed *h-Z* mathematical model provides a simple yet efficient alternative to more complex *ad-hoc* algorithms for problems presenting either shocks or drying–wetting areas.

The performance of the proposed approach has been assessed using a set of examples representative of the type of problems of interest.

ACKNOWLEDGEMENTS

The authors gratefully acknowledge the support of the European Union (Project LAMÉ, ENV4-CT97-0619).

REFERENCES

1. Donea J. A Taylor–Galerkin method for convective transport problems. *International Journal for Numerical Methods in Engineering* 1984; **20**:101–109.
2. Peraire J. A Finite Element Method for Convection Dominated Flows. PhD thesis, University of Wales, Swansea, 1986.

3. Peraire J, Zienkiewicz OC, Morgan K. Shallow water problems. A general explicit formulation. *International Journal for Numerical Methods in Engineering* 1986; **22**:547–574.
4. Zienkiewicz OC, Codina R. A general algorithm for compressible and incompressible flow—Part I. The split, characteristic-based scheme. *International Journal for Numerical Methods in Fluids* 1995; **20**:869–885.
5. Zienkiewicz OC, Nithiarasu P, Codina R, Vazquez M, Ortiz P. The characteristic-based-split procedure: An efficient and accurate algorithm for fluid problems. *International Journal for Numerical Methods in Fluids* 1999; **31**:359–392.
6. Zienkiewicz OC, Ortiz P. A split-characteristic based finite element model for the shallow water equations. *International Journal for Numerical Methods in Fluids* 1995; **20**:1061–1080.
7. Fraccarollo L, Toro EF. Experimental and numerical assessment of the shallow water model for two-dimensional dam-break type problems. *Journal of Hydraulic Research* 1995; **33**:843–864.
8. Zoppou C, Roberts S. Catastrophic collapse of water supply reservoirs in urban areas. *Journal of Hydraulic Engineering* 1999; **125**(7):686–695.
9. Wang JS, Ni HG, He YS. Finite-difference TVD scheme for computation of dam-break problems. *Journal of Hydraulic Engineering* 2000; **126**(4):253–262.
10. Brufau P, García-Navarro P. Two-dimensional dam break flow simulation. *International Journal for Numerical Methods in Fluids* 2000; **33**:35–57.
11. Satya Sai BVK, Zienkiewicz OC, Manzari MT, Lyra PRM, Morgan K. General purpose versus special algorithms for high-speed flows with shocks. *International Journal for Numerical Methods in Fluids* 1998; **27**:57–80.
12. Zienkiewicz O. Personal communication.
13. Zienkiewicz OC, Taylor RL. *The Finite Element Method*, vol. 2, McGraw-Hill, 1991.
14. Toro E. *Riemann Solvers and Numerical Methods for Fluid Dynamics. A Practical Introduction*, 2nd edn. Springer-Verlag: Berlin, 1999.
15. Rickenmann D, Koch T. Comparison of debris flow modelling approaches. In Chen C-L (ed), *Debris-Flow Hazards Mitigation*: *Mechanics*, *Prediction and Assessment. Proc.1st Int.Conference*, pp. 576–585. ASCE, 1997.
16. Donea J, Giuliani S, Laval H, Quartapelle L. Time accurate solution of advection–diffusion problems by finite elements. *Computer Methods in Applied Mechanics and Engineering* 1984; **45**:123–145.
17. Richtmyer RD, Morton KW. *Difference Methods for Initial Value Problems*, 2nd edn. John Wiley & Sons: New York, 1967.
18. Hirsch C. *Numerical Computation of Internal and External Flows*, vol. 2. John Wiley & Sons: Chichester, 1990.
19. Lynch PR, Gray WG. Finite element simulation of flow in deforming regions. *Journal of Computational Physics* 1980; **36**:135–153.
20. Sethian J. *Level Set Methods. Evolving Interfaces in Geometry*, *Fluid Mechanics*, *Computer Vision*, *and Material Science*. Cambridge University Press: Cambridge, 1996.
21. Sussman M, Smereka P, Osher S. A level set approach for computing solutions to incompressible two-phase flow. *Journal of Computational Physics* 1994; **114**:146–159.
22. Quecedo M, Pastor M. Application of the level set method to the finite element solution of two-phase flows. *International Journal for Numerical Methods in Engineering* 2001; **50**:645–663.
23. Mohapatra VEPK, Bhallamudi S. Two-dimensional analysis of dam-break flow in vertical plane. *Journal of Hydraulic Engineering* 1999; **125**(2):183–192.
24. Alcrudo F, García-Navarro P. A high resolution Godunov-type scheme in finite volume for the shallow water equations. *International Journal for Numerical Methods in Fluids* 1991; **16**:489–505.

